Novel Swirl-Flow Reactor for Kinetic Studies of Semiconductor Photocatalysis

Ajay K. Ray and Antonie A. C. M. Beenackers
Dept. of Chemical Engineering, University of Groningen, 9747 AG Groningen, The Netherlands

A new two-phase swirl-flow monolithic-type reactor was designed to study the kinetics of heterogeneous photocatalytic processes on immobilized semiconductor catalysts. True kinetic rate constants for destruction of a textile dye were measured as a function of wavelength of light intensity and angle of incidence, catalyst layer thickness, and the effect of absorption of light by liquid film on the overall rate of photocatalytic degradation. Photocatalytic activities of two commercially available TiO_2 catalysts (Degussa P25 and Hombikat UV 100) were also compared for different light intensities and catalyst layer thickness. Residence time distribution and mass-transfer limitations were evaluated. This new reactor appears to be an attractive choice for kinetic studies of heterogeneous photocatalysis.

Introduction

Heterogeneous photocatalysis has received considerable attention in years as an alternative for treating water polluted with hazardous organic chemicals (Fox and Dulay, 1993; Hoffmann et al., 1995). The process couples low-energy ultraviolet light with semiconductors acting as photocatalysts overcoming many of the drawbacks that exist for the traditional water treatment methods (Mills et al., 1993). Also, the photocatalytic process has the advantage (Matthews, 1992) of complete breakdown of organic pollutants to yield CO_2, H_2O, and mineral acids. Practically any organic pollutants can be completely mineralized by this process into harmless substances, including aliphatics, aromatics, polymers, dyes, surfactants, pesticides, and herbicides (Ollis et al., 1991). Often (Legrini et al., 1993; Mills et al., 1993) an aqueous suspension of catalyst particles in immersion or annular-type photoreactors has been used. Depending on the means of agitation the photoreactor resembled that of slurry or fluidized bed reactors. However, the use of suspensions requires the separation and recycling of the ultrafine catalyst from the treated liquid that is usually an inconvenient, time-consuming expensive process.

A novel semibatch swirl-flow monolith-type reactor was designed to study the kinetics of photocatalytic reactions. Monoliths are unique catalyst supports that provide a high surface-to-volume ratio and allow high flow rates with low pressure drop. The catalyst was immobilized for continuous use and to eliminate the need of separation for postprocess treatment. Experiments were performed to determine the various rate constants. Experiments were conducted to study the effect of light intensity and catalyst-layer thickness on reaction rate constant, the effect on overall reaction rate when light has to travel through the scattering, and absorbing heterogeneous medium to activate catalyst and the effect of angle of incidence of light falling on catalyst particles. As evident for most fixed-catalyst systems, mass-transfer limitations do exist. These were measured and results were corrected to obtain pure kinetic data. In this article, fundamental experimental kinetic data on photocatalytic oxidation of a textile dye was investigated under conditions that are relevant for evaluation of the design of other reactors.

Experimental Details

Experimental setup

The reactor consists of two circular glass plates, each of diameter 0.095 m, that are placed between soft padding housed within stainless-steel and aluminum casings separated by 2.9×10^{-3} m (Figure 1). The catalyst was deposited either on top of the bottom plate or on the bottom of the top plate. The polluted water was introduced tangentially between the two glass plates, and exited from the center of the top plate. The tangential introduction of liquid created a swirl-flow,

Present address of Ajay K. Ray: Department of Chemical Engineering, National University of Singapore, 10 Kent Ridge Crescent, Singapore 119260.

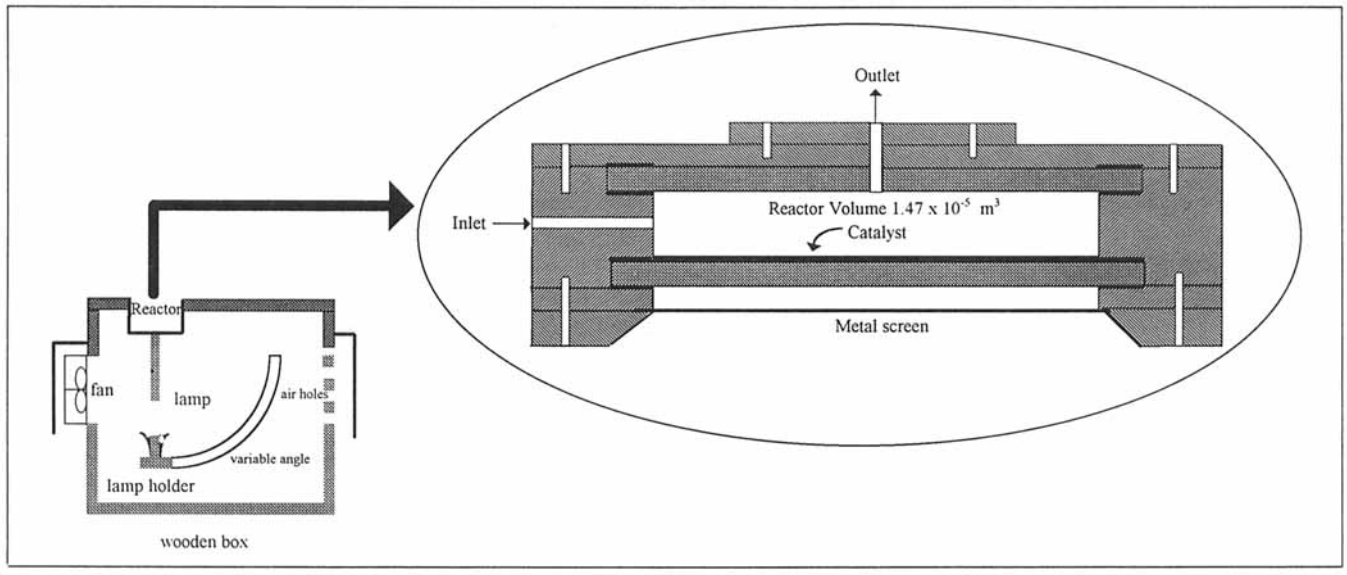

Figure 1. Reactor setup.

thereby minimizing mass transfer of pollutants to the catalyst surface. The lamp (Philips HPR 125 W high-pressure mercury vapor) was placed 0.07 m underneath the bottom glass plate on a holder that could be moved to create a different angle of incidence of light on the catalyst plate. The lamp and reactor were placed inside a wooden box painted black so that no stray light can enter into the reactor. The lamp was constantly cooled by a fan to keep the temperature down and protect the lamp from overheating. The lamp has a spectral energy distribution with a sharp peak at $\lambda = 365.5$ nm of 2.1 W, and thereby the incident light intensity was 213 W/m^2. Provision was made for placement of several metal screens of different mesh size between the lamp and bottom glass plate to obtain variation in light intensity. The effective surface areas of the catalyst that is illuminated and the volume of the reactor are 5.027×10^{-3} m^2 and 1.47×10^{-5} m^3, respectively. For the reactor κ, defined as the ratio of illuminated surface area of catalyst that is in contact with reaction liquid per m^3 of liquid treated within the reactor volume equals 342 m^2/m^3.

A gear pump (Verder model 2035 with a maximum flow rate of 4.0×10^{-6} m^3/s) was used for pumping the reactant between the reactor and the reservoir via a bottom-loader flowthrough cuvette (Hellma; quartz, path length 0.001 m) placed inside a spectrophotometer for continuous on-line measurement of the model component (Figure 2). Two three-way glass valves were used between the water and specially designed reactant reservoir for initial zero setting of the analytical instrument before the start of an experiment, introduction of the reactant into the system, elimination of bubbles formed during experiment, and final flushing of the entire system.

Catalyst

Degussa P25 grade TiO_2 was used for most of the experiments without further treatment. It has a BET surface area of $(5.5\pm1.5)\times10^4$ m^2/kg and crystallite sizes of 30 nm in 0.1-μm-diameter aggregates. A few experiments were also performed with Hombikat UV 100 (Sachtleben Chemie, Germany) to compare the photocatalytic activity of the two catalysts. The specifications of the two catalysts are compared in Table 1.

Catalyst immobilization

Pyrex roughened by sand blasting for improved catalyst fixation, was chosen as the support material since it is transparent to UV radiation down to a wavelength of about 300 nm. The glass surface was carefully degreased, cleaned with 5% HNO_3 solution overnight, washed with water, and then dried at 393 K. A 5% aqueous suspension of the catalyst was prepared with water out of a Millipore Milli-Q water purification system. The suspension was mixed in an ultrasonic cleaner (Branson 2200) bath for 1,800 s to obtain a milky

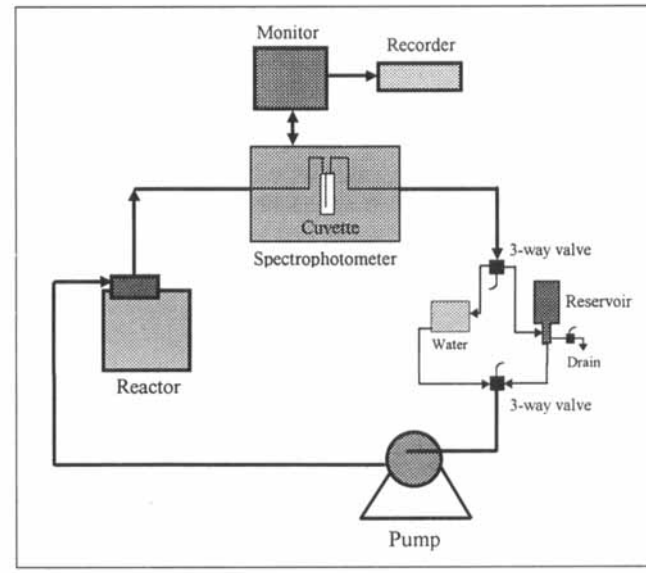

Figure 2. Experimental setup.

Table 1. Comparison of Two Different Commercial TiO_2 Catalysts

Specifications/Catalyst	Degussa P25	Hombikat UV100
Crystal phase	70:30 anatase	100% anatase
Particle size, nm	30	< 10
BET surface area, m^2/g	55 ± 15	> 250

suspension that remained stable for weeks. The substrate was then coated with catalyst by inserting it into the suspension and pulling it out slowly by the dip-coating technique (Chopra et al., 1983). The catalyst coating was dried at 393 K for 1,800 s and then calcined in a furnace (Heraeus UT 6060) in a vertical position by raising the temperature gradually at a rate of 0.15 K/s (to avoid cracking of the film) to a final firing temperature of 573 K and held there for 3 h. The total amount of catalyst deposited per unit area was determined by weighing the glass plate before and after the deposition. Depending on the number of dipping, the amount of catalyst obtained was between 5.0×10^{-4} and 3.5×10^{-3} kg/m^2.

Model component

The model component used for kinetic studies was a brightly colored water-soluble acid dye Special Brilliant Blue (MW 812), SBB, laboratory reagent grade (in 20% solution), which was obtained from Bayer (catalogue number 42735). This is an excellent model component for characterization of a photocatalytic reactor (Assink et al., 1993), and this dye is reactive only in the presence of both TiO_2 and UV light, is biologically not degradable, and is found in wastewater from the textile industry.

Analysis

Changes in SBB dye concentration were measured on-line with a flowthrough curvet (Hellma quartz cuvet of path length 1 cm) inside a spectrophotometer (Philips PU8700 UV-VIS), and was recorded continuously. Calibration curves were prepared using solutions of known concentration with an analytical wavelength of 605 nm. For concentrations up to 0.5 mol/m^3 the Beer–Lambert law was obeyed with good precision and the absorptivity coefficient, ϵ (at $\lambda_{max} = 605$ nm), was found to be 5,000 $m^3/mol/m$. The light intensity was measured by a digital radiometer (UVP Model number UVX-36).

Experimental procedure

Before placing the catalyst plate inside the reactor, the light intensity on the top of a bare glass plate was measured with the digital radiometer. At the start of every experiment the reactor was filled with Milli-Q water and rinsed several times before zero-setting the analytical instrument. The reactor and connecting lines were then filled with the dye solution, and it was ensured that no air bubbles remained in the system. The change in the dye concentration was continuously analyzed and recorded. New silicon connecting tubes and catalyst plate were found to adsorb the dye for about an hour, but no noticeable adsorption by the entire system was observed afterwards. Light was turned on only when the spectrophotometer reading was stabilized. At the end of the experiment the entire system was rinsed with Milli-Q water, catalyst plate was removed, dried, and weighed again to determine any loss of catalyst during experimentation.

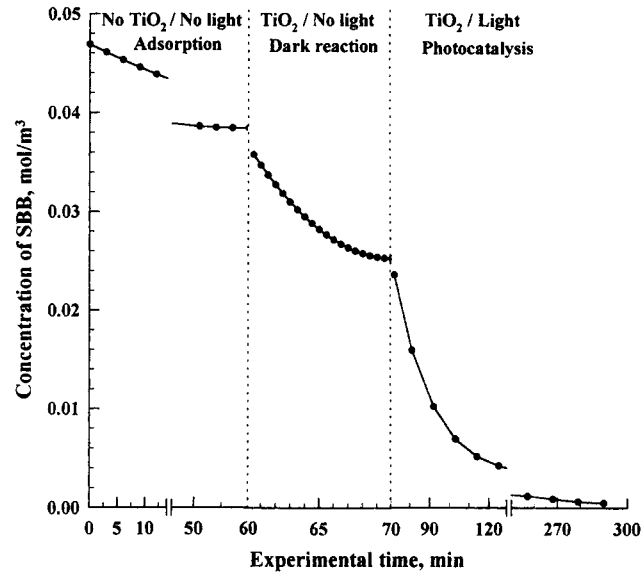

Figure 3. Typical experimental run showing dye adsorption by the system, dark reaction, and photocatalytic reaction.

A typical experimental result is shown in Figure 3. The decrease in concentration in the first part is attributed to the adsorption of the dye by the connecting tubing (no catalyst present), while that of the second part is due to adsorption of the dye onto fresh catalyst plate (dark reaction). The decrease in the last part is when light is turned on and actual photocatalysis occurred. Concentrations decrease like that of the first two parts was observed only when new tubing or fresh catalyst plate was used. However, before turning the light on, we always made sure that the reading was constant in the spectrophotometer.

Results and Discussion

Residence time distribution

Residence time distribution (RTD) was measured by instantaneous pulse injections of the dye in the reactor containing no catalyst and measuring continuously the outlet concentration spectrophotometrically. The E-curve from a typical experimental run ($C_0 = 0.275$ mol/m^3; $Q = 1.88 \times 10^{-6}$ m^3/s) is shown in Figure 4. The resulting mean residence time, t_{mean}, and the standard deviation, σ, were calculated as 7.7 s and 7.1 s, respectively. Although from the distribution in the graph it is apparent that there is a high degree of mixing, a close scrutiny of the distribution reveals that about 64% of the tracer dye is coming out before the mean residence time (channeling) and that the distribution has a long tail suggesting the existence of dead volume space. A two-parameter model was used to describe the reactor as an ideally mixed zone of volume αV, a dead zone of volume $(1-\alpha)V$, and a shortcut bypass stream of flow rate $(1-\beta)Q$ (Fogler, 1986). For this flow rate ($Q = 1.88 \times 10^{-6}$ m^3/s), α and β were found to be 0.877 and 0.67, while the Peclet number, Pe, from the dispersion model and N, the number of tanks re-

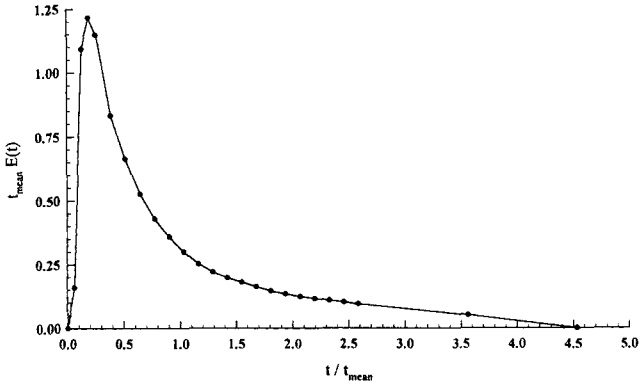

Figure 4. RTD for a pulse input.

$V_R = 1.47 \times 10^{-5}$ m^3; $Q = 1.88 \times 10^{-6}$ m^3/s; input tracer concentration = 0.275 mol/m^3; $t_{mean} = 7.7$ s, $\sigma = 7.1$ s; $Pe = 0.525$ (dispersion model); $N = 1.42$ (tank-in-series model); fraction exiting before mean time = 0.64; dead volume fraction, $(1 - \alpha) = 0.123$; bypass fraction, $(1 - \beta) = 0.33$.

quired, from the tanks-in-series model, were found to be 0.525 and 1.42, respectively.

Flow Characterization. The flow pattern inside a reactor of the same dimension was calculated by solving momentum equations using a commercial software package, FLUENT. In Figure 5, particle trajectory is shown for an inlet flow rate of 1.88×10^{-6} m^3/s. The figure shows that tangential introduction of fluid indeed creates swirl-flow inside the reactor. It also reveals the presence of a dead zone in the lower right corner and bypassing of fluid commensurate with the results obtained from RTD experiments.

Rate Expressions. Heterogeneous photocatalytic degradations are often Langmuir–Hinshelwood kinetics (Ollis et al., 1989; Mills et al., 1993). For our system, the intrinsic reaction rate, R, could be

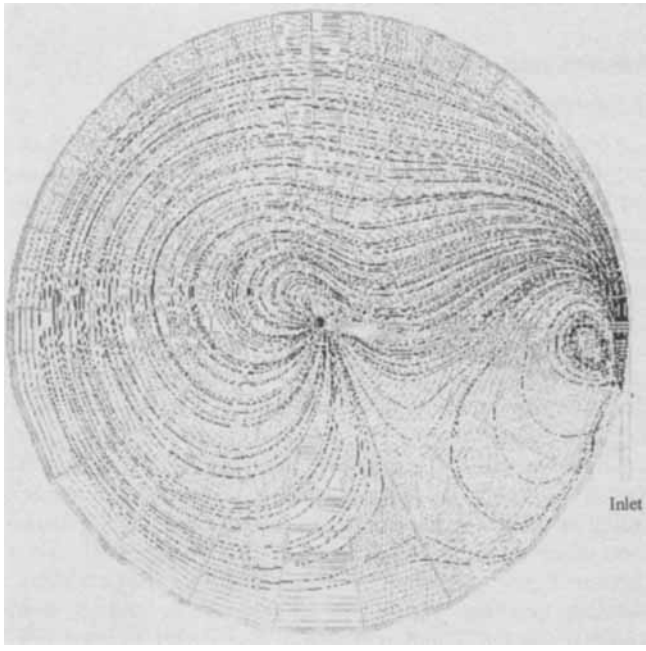

Figure 5. Flow pattern inside the novel reactor.

$$R = \left[\frac{V_L}{\kappa V_R}\right]\left(-\frac{dC}{dt}\right) = \frac{kKC_S}{1 + KC_S}, \quad (1)$$

where V_L and V_R are the total volume of liquid treated and volume of reactor (m^3), respectively; κ is the illuminated specific surface area of catalyst in contact with reaction liquid inside the reactor (m^2/m^3); dC/dt is the observed rate (mol/m^3/s); k and K are the reaction rate constant (mol/m^2/s) and adsorption equilibrium constant (m^3/mol), respectively; and C_S is the concentration of the reactant at the catalyst surface (mol/m^3) in equilibrium with the actual surface concentration. For practical reasons, R is expressed as moles reacted per unit time per unit illuminated area of catalyst, rather than per unit active sites or per unit mass of the catalyst. Rates expressed per unit active sites are scientifically more appealing, but these are difficult to measure. Defining R on the total mass of catalyst is not practical because of the uncertainty of the extent to which the catalyst is active, especially when it is immobilized.

Influence of external mass transfer

For evaluation of fundamental kinetic parameters it is necessary to eliminate mass-transfer resistance. At steady state the conversion rate follows from

$$N = k_m(C_0 - C_s) = \frac{kKC_s}{1 + KC_s}, \quad (2)$$

where C_0, C_s are the concentration in the bulk and close to the catalyst surface, respectively; k_m is the mass-transfer rate. k_m was determined experimentally by measuring the dissolution rate of benzoic acid, coated at the inside of the bottom glass plate, into water flowing at different flow rates ($C_{out}/C_{sat} \approx 0.04$). The result is shown in Figure 6 as a function of the Reynolds number, together with the best fit:

$$k_m = 6.1 \times 10^{-7}\,[Re]^{0.62}. \quad (3)$$

All subsequent experiments performed were at a flow rate of 1.88×10^{-6} m^3/s, as a higher flow rate introduces bubbles inside the reactor. Reynolds number and k_m values corre-

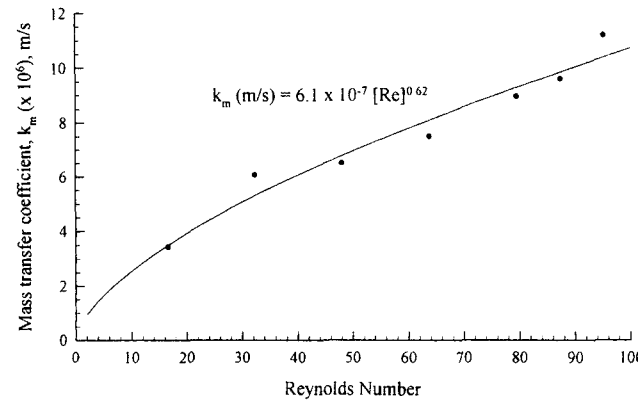

Figure 6. Measurement of mass-transfer coefficient, k_m, with Reynolds number, Re.

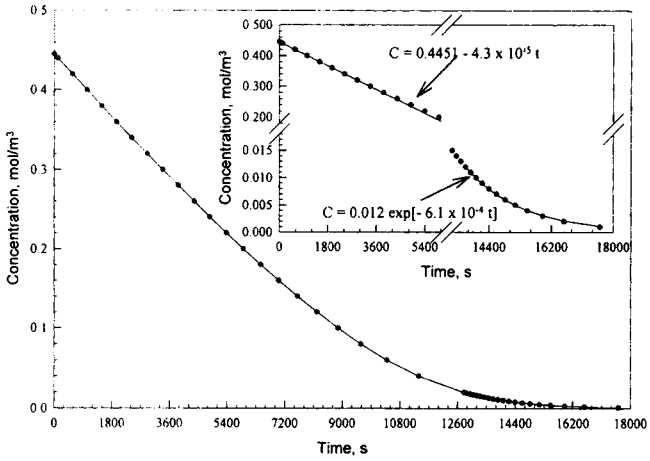

Figure 7. Calculation of rate constants.

SC illumination; $Q = 1.88 \times 10^{-6}$ m³/s; $I = 50$ W/m²; $V_L = 2.8 \times 10^{-5}$ m³; $w = 2.59 \times 10^{-3}$ kg/m²; solid line: model fit with Eqs. 1, 2, and 3.

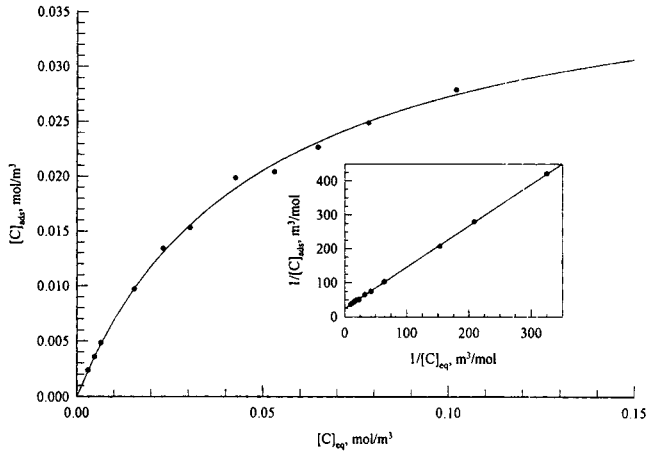

Figure 8. Calculation of adsorption rate constant from dark reaction.

SC illumination; $Q = 1.88 \times 10^{-6}$ m³/s; $V_L = 2.9 \times 10^{-5}$ m³; $w = 2.6 \times 10^{-3}$ kg/m².

sponding to this flow rate are 91 and 9.99×10^{-6} m/s. Knowing k_m, values of C_s could be calculated from Eq. 2 and, subsequently, true kinetic parameters, k and K, were evaluated.

Calculation of Rate Constants. The rate constants k and K were found from a photocatalytic degradation experiment starting with a high initial concentration and then fitted with the model equation described in Eqs. 1 and 2 by the Levenberg–Marquardt method (Seber and Wild, 1989). The k_m value used was from Eq. 3. Figure 7 shows the result of a photocatalytic experiment with a high initial dye concentration. In agreement with Eqs. 1 and 2, k and K are given as 0.31 μmol/m²/s and 18.49 m³/mol, respectively.

Dark reaction

The small rapid decrease in dye concentration in the absence of light (dark reaction) when a fresh catalyst plate was used can be attributed to the adsorption of the dye onto the catalyst (second part of Figure 3). The concentration of dye adsorbed on the surface can be calculated from the difference between the initial and equilibrium (no more decrease with time) concentrations. When the results are plotted (Figure 8), it appeared to follow a Langmuir adsorption isotherm:

$$[C]_{ads} = \frac{NK[C]_{eq}}{1 + K[C]_{eq}} \tag{4}$$

where $[C]_{ads}$ and $[C]_{eq}$ are the concentration of dye adsorbed and the equilibrium concentration of dye used, respectively; N and K are the saturation and adsorption equilibrium value, respectively. When the data were fitted with Eq. 4 by the Marquardt–Levenberg method (Seber and Wild, 1989), N and K were found to be 0.0405 mol/m³ and 20.41 m³/mol, respectively. Figure 8 also shows the experimental results in the form of $1/[C]_{ads}$ vs. $1/[C]_{eq}$. When the data were fitted with a straight line, N and K were found to be 0.0416 mol/m³ and 19.7 m³/mol, respectively, from the slope and intercept of the plot. This appeared to be within 10% of the value obtained from the photocatalytic experiments, thus suggesting that K indeed represents adsorption characteristics.

Effect of Light Intensity. The reaction rate constant, k, usually follows power-law dependence on light intensities (Ollis et al., 1989). Light intensity falling on the catalyst was varied when different mesh-size metal screens were placed between the lamp and the catalyst. k was measured as a function of I, keeping all other parameters fixed. Figure 9 shows experimental values for the catalyst on the bottom plate. A fit in the form of

$$k(I) = a[I]^b \tag{5}$$

was not very good (dotted line), and the value of the exponent obtained was 0.21 instead of the value between 0.5 and 1 reported in the literature (Ollis et al., 1991). However, a correlation in the form of

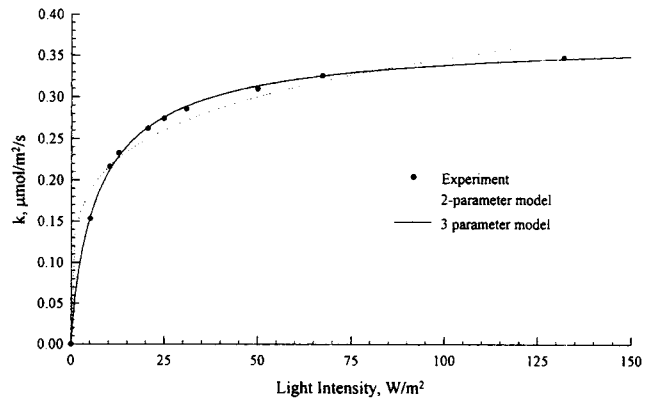

Figure 9. Effect of light intensity of rate constant, k.

SC illumination; $Q = 1.88 \times 10^{-6}$ m³/s; $V_L = 2.8 \times 10^{-5}$ m³; $w = 2.6 \times 10^{-3}$ kg/m²; $C_0 = 0.029$ mol/m³; 2-parameter model (Eq. 5): $a = 0.1345$, $b = 0.205$; 3-parameter model (Eq. 6): $k_s = 0.376$ μmol/m²/s, $a = 0.176$, $b = 0.85$.

$$k(I) = \frac{k_s a[I]^b}{1 + a[I]^b} \tag{6}$$

appeared to fit the data exceptionally well (solid line), with k_s, a, and b as 0.38, 0.18, and 0.85, respectively.

Effect of Absorption of Light by the Model Component. Experiments were carried out with the catalyst present on both the bottom plate and the top plate. In the latter case, the light intensity on the catalyst surface was considerably reduced, as it has to travel through the absorbing liquid. The two cases are depicted as *SC* (substrate–catalyst) and *LC* (liquid–catalyst), respectively. For results, see Figure 10. The *SC* illumination case is fitted to the theoretical expressions of

$$R_i = \frac{kKC_{S,i}}{1 + KC_{S,i}} \tag{7}$$

using k and K values of 0.29 μmol/m^2/s (from Eq. 6 with $I = 30.5$ W/m^2) and 18.5 m^3/mol, respectively. For the *LC* illumination, k was calculated from Eq. 6 using intensity, I, values corrected for absorption from the well-known Lambert–Beer's law

$$\log\left[\frac{I_0}{I}\right] = \epsilon b C. \tag{8}$$

The model fit (solid lines) explains that the reduction of the degradation rate for the *LC* illumination is primarily due to the absorption of the light by the model component. Figure 10 also reveals that in the scale-up of the photocatalytic reactor, one must comply with the fact that the degradation rate will be severely affected and the reactor size will be constrained by the phenomena of opacity, light scattering, depth of penetration, and local volumetric light absorption.

Effect of Angle of Incidence of Light. A study of the dependence of the rate with variations in the angle of incidence is of interest with respect to the novel reactor configurations studied by us. The lamp was placed 0.07 m below the reactor on a holder that could be moved to create different angles of incidence of light on the catalyst. The lamp and the reactor were placed inside a wooden box painted black to prevent

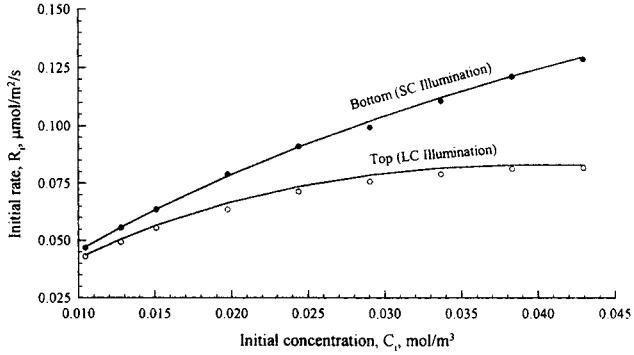

Figure 10. Effect of absorption of light by dye on photocatalytic degradation rate.

$Q = 1.88\times10^{-6}$ m^3/s; $V_L = 2.8\times10^{-5}$ m^3; $w = 2.6\times10^{-3}$ kg/m^2; $I = 30.5$ W/m^2; solid lines ≡ model fit; for Eq. 8: $b = 2.9\times10^{-3}$ m, $\epsilon = 5000$ m^2/mol.

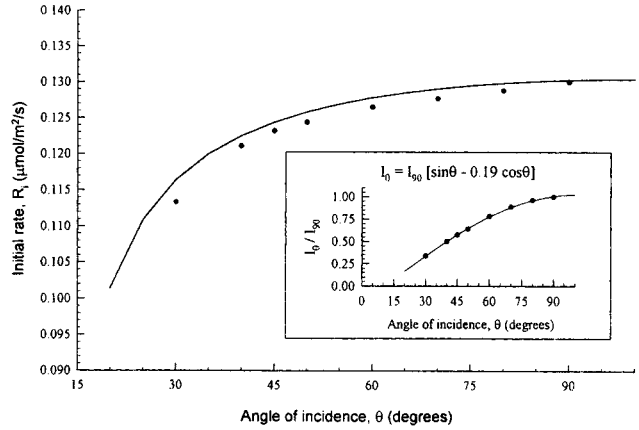

Figure 11. Effect of angle of incidence of light on photocatalytic degradation rate and on light intensity on catalyst.

SC illumination; $Q = 1.88\times10^{-6}$ m^3/s; $V_L = 2.8\times10^{-5}$ m^3; $w = 2.58\times10^{-3}$ kg/m^2; $C_0 = 0.032$ mol/m^3.

stray light from entering the reactor. Figure 11 shows the experimental results (filled circle) of the effect of the angle of incidence of the light on the photocatalytic degradation rate. In the figure 90° represents the angle when the lamp is directly below the catalyst plate. As expected, the rate decreased when the lamp was moved away from the vertical position. The variation of light intensity with the angle of incidence was measured with a digital radiometer and is also shown in Figure 11. The experimentally measured value was fitted with an expression in the form of

$$I_\theta = I_{90}[\sin\theta + a\cos\theta], \tag{9}$$

where I_θ and I_{90} are the intensity at angle θ and 90°, respectively, and a is a constant. The sine term represents the component of light intensity falling directly on the catalyst, whereas the cosine term comes from the light reaching the catalyst through back scattering from the box wall. The variation in the experimental rate with the angle of incidence was then fitted (solid line) with a model described by Eq. 7, using k values calculated from Eqs. 6 and 9. The model fits the experimental data reasonably well.

Effect of Amount of Catalyst. Variation in the catalyst thickness was obtained by immobilizing the different layers of catalyst onto the plate and measuring the amount by difference in weight in a μg-sensitive balance. Our results varied between 5.0×10^{-4} and 3.5×10^{-3} kg/m^2, and therefore the optical film thickness, based on a 100% dense film, varied between 0.1 μm and 1.0 μm. Since the films were certainly not 100% dense, the actual thickness would be somewhat higher. Figure 12 shows scanning electron micrograph pictures illustrating the surface morphology of a roughened (sand blasted) glass plate with no catalyst, and TiO_2 films containing 5.0×10^{-4} and 3.0×10^{-3} kg/m^2.

Figures 13 and 14 show the experimental results of the initial degradation rate with the amount of catalyst for varying light intensity when the catalyst was present on the bottom (*SC* illumination) and the top (*LC* illumination), respectively. The difference in the R_i values between the Figures

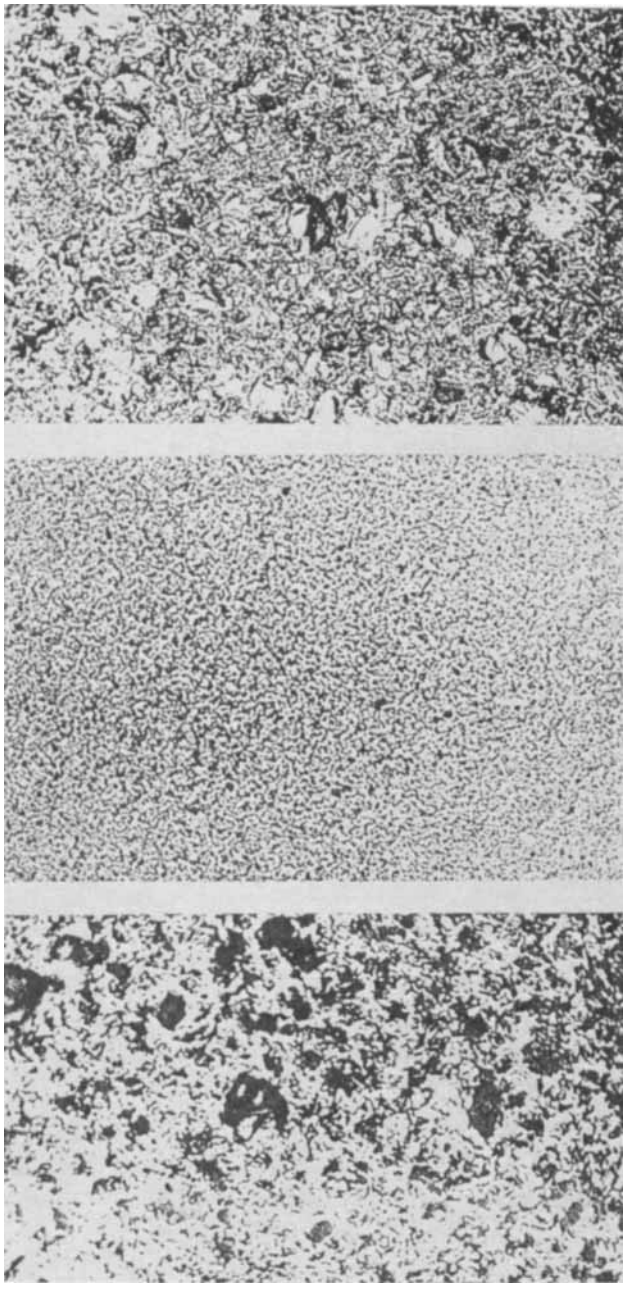

Figure 12. Scanning electron micrographs showing TiO_2 films deposited on glass.

(a) Roughened glass surface with no catalyst. (b) Thin film (5.0×10^{-4} kg/m^2) of TiO_2. (c) Thick film (3.0×10^{-3} kg/m^2) of TiO_2.

13 and 14 is due to the reduction in the light intensity by the presence of a light-absorbing dye and is discussed earlier. The figures show that the photocatalytic degradation rate increases with the amount of catalyst, w, up to a maximum value. Apparently, the amount of catalyst should be limited to about 0.003 kg/m^2 because only marginal improvement in the degradation rate beyond the preceding value is observed, whereas, from the thick layer, the catalyst appeared to wash away more readily.

The effect of w was modeled by trying a relation in the form of:

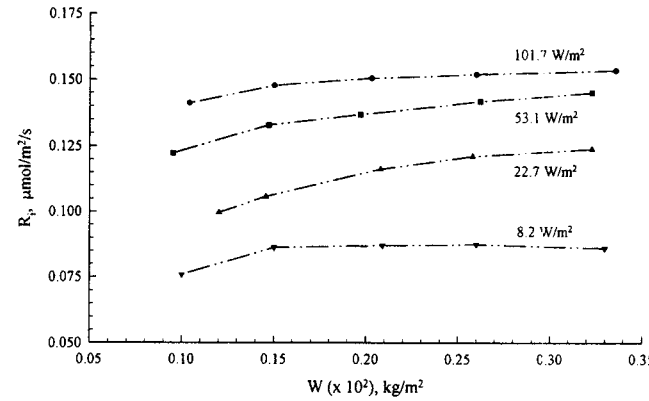

Figure 13. Effect of amount of catalyst on degradation rate.

SC illumination; $Q = 1.88\times10^{-6}$ m^3/s; $V_L = 2.8\times10^{-5}$ m^3; $C_0 = 0.043$ mol/m^3.

$$a = a'[w]^n \tag{10}$$

with a the constant from Eq. 6. The best fits were obtained for $n = 0.5$, resulting in an extension of Eq. 6 as follows:

$$k(I,w) = \frac{k_s a'(\sqrt{w})I^b}{1 + a'(\sqrt{w})I^b}, \tag{11}$$

where the values of constants k_s, a', and b are 0.38, 3.45, and 0.85, respectively, and the values of k, I, and w are expressed as μmol/m^2/s, W/m^2, and kg/m^2, respectively.

Comparison of Photocatalytic Activities of Two Different Commercial TiO_2 Samples. Recently, a new TiO_2 catalyst with the brand name of Hombikat UV 100 has been claimed by Sachtleben Chemical (Germany) to be more active than Degussa P25. This may be due to its particle size being smaller and thus, the surface area that is availale for reaction is larger (Table 1). Figure 15 compares the experimental results of *SC* illumination for both of the catalysts. The figure shows that Hombikat UV100 is photocatalytically more active than De-

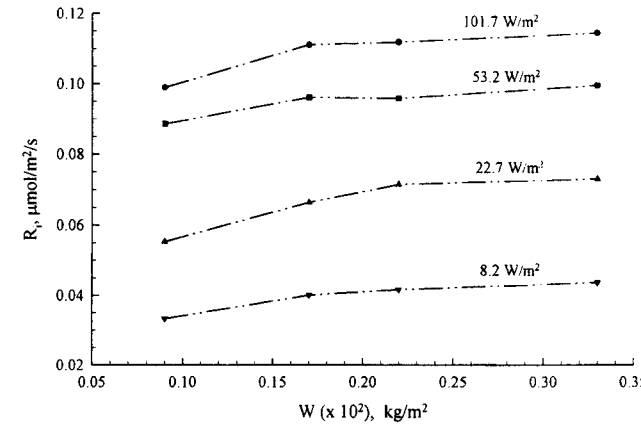

Figure 14. Effect of amount of catalyst on degradation rate.

SC illumination; $Q = 1.88\times10^{-6}$ m^3/s; $V_L = 2.8\times10^{-5}$ m^3; $C_0 = 0.033$ mol/m^3.

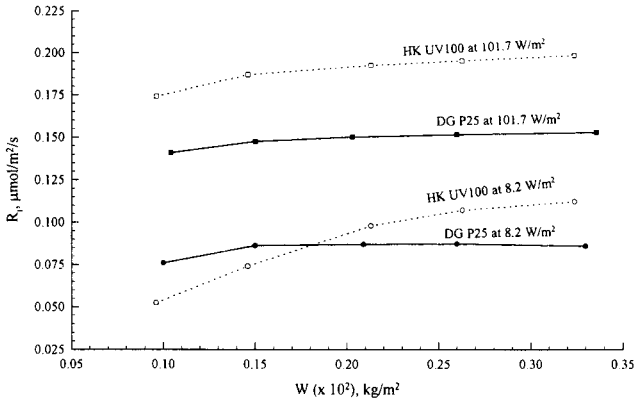

Figure 15. Comparison of activity of Degussa P25 and Hombikat UV100 as a function of the amount of catalyst and light intensity.

SC illumination; $Q = 1.88 \times 10^{-6}$ m³/s; $V_L = 2.8 \times 10^{-5}$ m³; $C_0 = 0.043$ mol/m³.

gussa P25 in all cases except for thin layers at low light intensities.

Conclusions

A new swirl-flow monolithic-type semibatch reactor was designed and used to evaluate kinetic parameters for photocatalytic degradation of a textile dye. The design is unique for the kinetic study of semiconductor photocatalysis, as it can be used to measure, apart from various rate constants, the effects of the catalyst layer thickness, light intensity, and angle of incidence on the reaction rate constants when it falls directly on the catalyst or when it has to travel through absorbing and scattering liquid media.

The residence time distribution of the liquid phase within the reactor was determined, and calculated values of the distribution parameters and Peclet number reveal that the liquid phase was substantially well mixed. The photocatalytic rates reported in this article for the model component SBB with the Degussa P25 catalyst can be described by the following equation

$$R = k_m(C_0 - C_S) = \frac{k[I(\theta), w]KC_s}{1 + KC_s},$$

where

$$k_m = 6.1 \times 10^{-7}[Re]^{0.62} \quad \text{for} \quad Re < 100$$

$$k[I(\theta), w] = \frac{k_s a'(\sqrt{w})[I(\theta)]^b}{1 + a'(\sqrt{w})[I(\theta)]^b}$$

$$k_s = 0.38\ \mu\text{mol/m}^2\text{/s}; \quad a' = 3.45;$$

$$b = 0.85; \quad K = 18.5\ \text{m}^3\text{/mol}$$

$$I(\theta) = I_{90}[\sin\theta - 0.19\cos\theta] \quad \text{for} \quad 30° < \theta < 90°$$

$$5.0 \times 10^{-4} < w\ (\text{kg/m}^2) < 3.5 \times 10^{-3}; \quad I_{90} < 200\ \text{W/m}^2$$

An increase in photoactivity of 20–30% was obtained for the Hombikat UV100 catalyst over Degussa P25 for all cases except for experiments performed with thin layers of catalyst at low light intensity.

The reactor appears to be an attractive choice for procuring kinetic data for different model components and for determining the dependence of various parameters on the photocatalytic degradation rates.

Acknowledgments

We acknowledge the financial support from the Netherlands ministry of Economic Affairs, The Hague. We thank Hetty Hoffstinge and Jan Reitsma for experimental work and Luuk Balt for technical assistance.

Notation

N = flux, mol/m²/s
κ = illuminated catalyst density, m²/m³
λ = wavelength, nm

Subscripts and superscripts

0 = initial
i = initial
s = substrate; saturation

Literature Cited

Assink, J. W., T. P. M. Koster, and J. M. Slaager, "Fotokatalytische Oxydatie voor Afvalwaterbehandeling," Internal Rep., TNO-Milieu en Energie, Apeldoorn, The Netherlands (1993).

Chopra, K. L., S. Major, and D. K. Pandya, "Transparent Conductors—A Status Review," *Thin Solid Films*, **102**, 1 (1983).

Fogler, H. S., *Elements of Chemical Reaction Engineering*, Prentice Hall, Englewood Cliffs, NJ (1986).

Fox, M. A., and M. T. Dulay, "Heterogeneous Photocatalysis," *Chem. Rev.*, **93**, 341 (1993).

Hoffmann, M. R., S. C. Martin, W. Choi, and D. W. Bahnemann, "Environmental Applications of Semiconductor Photocatalysis," *Chem. Rev.*, **95**, 69 (1995).

Legrini, O., E. Oliveros, and A. M. Braun, "Photochemical Processes for Water Treatment," *Chem. Rev.*, **93**, 671 (1993).

Matthews, R. W., "Photocatalytic Oxidation of Organic Contaminants in Water: An Aid to Environmental Preservation," *Pure Appl. Chem.*, **64**(9), 1285 (1992).

Mills, A., R. H. Davies, and D. Worsley, "Water Purification by Semiconductor Photocatalysis," *Chem. Soc. Rev.*, 417 (1993).

Ollis, D. F., E. Pelizzetti, and N. Serpone, "Heterogeneous Photocatalysis in the Environment: Application to Water Purification," *Photocatalysis: Fundamentals and Applications*, Chap. 18, Wiley, New York, p. 603 (1989).

Ollis, D. F., E. Pelizzetti, and N. Serpone, "Destruction of Water Contaminants," *Environ. Sci. Technol.*, **25**(9), 1523 (1991).

Seber, G. A. F., and C. J. Wild, *Nonlinear Regression*, Wiley Interscience, New York (1989).

Manuscript received Mar. 10, 1997, and revision received June 2, 1997.